2011 50th IEEE Conference on Decision and Control and
European Control Conference (CDC-ECC)
Orlando, FL, USA, December 12-15, 2011

Two-Degree-of-Freedom LPV Control for a through-the-Road Hybrid Electric Vehicle via Torque Vectoring

Qin Liu, Gerd Kaiser, Sudchai Boonto, Herbert Werner, Frédéric Holzmann,
Benoît Chretien and Matthias Korte

Abstract— **This paper presents an application of linear-Parameter-Varying (LPV) control to solve the torque vectoring problem of a through-the-road hybrid electric vehicle (TtR-HEV). To achieve high performance both in reference tracking and disturbance rejection, a two-degree-of-freedom LPV self-scheduled controller is synthesized by using mixed sensitivity loop shaping. The controller is based on a single Lyapunov function and guarantees stability and a level of control performance for all admissible trajectories of varying parameters. Moreover, an anti-windup control scheme is derived by employing a two-step design procedure. Finally the designed controller is tested in various driving maneuvers and compared with a flatness-based controller.**

I. INTRODUCTION

Hybrid electric vehicles (HEV) are developed to achieve either better fuel economy or better performance, compared to conventional vehicles. Control schemes have been focused on the dual-axle propulsion system. The front-wheel axle and rear-wheel axle are separately driven, where one is propelled by a hybrid power train and the other one is driven by electric motors [1]. Moreover, regenerative braking on individual wheels can significantly improve the vehicle fuel efficiency and hence the fuel economy.

To overcome the conflict between stability and agility of the conventional vehicles, one emerging technique called torque vectoring is used in both pure electric and hybrid electric vehicles. Its benefits become more obvious, when the vehicle is commanded to drive along a curve, particularly at high vehicle speed. Due to the response time, that the vehicle takes to build up lateral forces on wheels, the vehicle responds slower than the expectations of drivers. Meanwhile, after a relatively long response time, the vehicle yaw movement, e.g. the yaw rate, presents overshoot and oscillation before settling on a steady state [7]. Conventional vehicle suspensions are tuned through bump steering, static settings, etc, to guarantee system stability at the expense of vehicle agility.

Adopting torque vectoring technique in a hybrid or pure electric vehicle enables independent control of each wheel. When the vehicle is cornering, the torques applied on the outside wheels are increased, while the inside wheels are effectively braked. Such a solution eliminates the need to compromise between response and stability.

Currently, torque vectoring receives enormous attention from car manufacturers for their next generation vehicles. In [7], an inverse model of the complex vehicle system is employed as the feedforward control part. Assuming the inverse model is an accurate representation of the actual system, it plays a significant role in the whole control scheme, where the feedback part is complementary to account for the external disturbances. However, this control concept lacks of generality, for it is not easy or even not possible to create a highly realistic model that represents the inverse of a complex non-linear vehicle. In [6], a combination of flat feedforward and LQG feedback controller is proposed in the application of torque vectoring. Its performance is demonstrated under extreme driving situations for reference tracking. Nevertheless, the construction of the flat nonlinear model involves the differentiation of measured signals [10], which may amplify measurement noise. An adaptive feedback linearization technique is proposed in [9] for an active front steering and rear torque vectoring vehicle in the presence of parameter uncertainties.

This paper presents a novel LPV self-scheduled control scheme to solve the torque vectoring problem of a through-the-road hybrid electric vehicle. A two-degree-of-freedom (2-DOF) controller is synthesized to realize the feedforward and feedback control simultaneously. It guarantees performance and stability for all admissible trajectories of varying parameters. Moreover, the feedforward and feedback controllers are synthesized in one optimization step.

In section 2 some facts about TtR-HEV are introduced for basic understanding. A single-track model to analyze vehicle lateral dynamics serves as the starting point before controller design. Section 3 focuses on the LPV model realization and self-scheduled controller synthesis. In section 4, the performance of the designed controllers is tested in different driving maneuvers in simulation, and compared with a controller proposed in [6]. Finally, conclusions are drawn in section 5.

II. THROUGH-THE-ROAD HYBRID ELECTRIC VEHICLE

To implement a hybrid power train, a natural way is to mount an electric drive train to an existing combustion engine driven propulsion system. Such an implementation is called through-the-road hybrid electric vehicle (TtR-HEV) [2]. The

This work was supported by the European Commission under Grant agreement no. 258133

Q. Liu, H. Werner are with the Institute of Control Systems, Hamburg University of Technology, Eissendorfer Str. 40, 21073, Hamburg, Germany {qin.liu, h.werner}@tu-harburg.de

G. Kaiser, F. Holzmann, B. Chretien, M. Korte are with Intedis GmbH, Delpstrasse 4, 97084 Wuerzburg, Germany gerd.kaiser@intedis.com

S. Boonto is with the department of Control System and Instrumentation Engineering, King Mongkut's University of Technology Thonburi, 10140, Thailand sudchai.boo@kmutt.ac.th

978-1-61284-799-3/11/$26.00 ©2011 IEEE

conventional combustion engine drives one axle, while the other one is equipped with electric components, including an electric energy storage and electric motors. Therefore, by assembling an internal combustion engine (ICE) driven vehicle with electric parts, together with necessary control units, a TtR-HEV is realized as in Fig. 1.

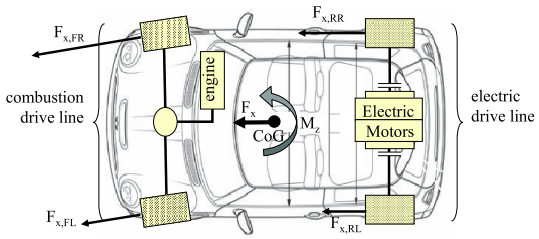

Fig. 1. Basic design of a TtR-HEV

This paper considers the electric drive designed in the way that two electric motors with their own controllers are mounted inside the wheels as hub motors. With the equipment of two motors, the size of the electric drive train is reduced and the final drive becomes unnecessary. Moreover, two independent motors make it possible, that torques are distributed to left and right wheels individually and in an optimal way.

A. Single-Track Model

Instead of working on complex vehicle models, considerable insight into the basic aspects of vehicle handling and stability can also be gained by taking a simplified model of a vehicle that runs at a constant speed over an even horizontal road. One well-known simplified vehicle model to be employed in this paper is a single-track model [8]. The second-order linearized vehicle lateral dynamics are written as follows:

$$\dot{\beta} = (\frac{-a_f C_f + a_r C_r}{m v_x^2} - 1)\dot{\psi} - \frac{C_f + C_r}{m v_x}\beta + \frac{C_f}{m v_x}\delta \qquad (1)$$

$$\ddot{\psi} = -\frac{a_f^2 C_f + a_r^2 C_r}{I_z v_x}\dot{\psi} + \frac{a_r C_r - a_f C_f}{I_z}\beta + \frac{a_f C_f}{I_z}\delta + \frac{1}{I_z}M_z \qquad (2)$$

Here the side slip angle β and yaw rate $\dot{\psi}$ are chosen as states for a state space realization. The driver's wish is described by the steering angle δ and longitudinal velocity v_x, both of which can be estimated or measured online. M_z is the generated yaw torque to turn the vehicle around the vertical axis, and is regarded as an input. $C_f, C_r, a_f, a_r, m, I_z$ are constant vehicle parameters and stand for the cornering stiffness of front wheel and rear wheel, distance from the center of gravity to the front axle and rear axle, vehicle mass, moment of inertia around the vertical axis, respectively (see Table I).

III. Torque Vectoring

A. LPV Model

An LPV state space model has the form:

$$G(\theta) := \left\{ \begin{array}{l} \dot{x} = A(\theta)x + B(\theta)u \\ y = C(\theta)x + D(\theta)u \end{array} \right. \qquad (3)$$

where $x \in \mathbb{R}^m$ is the state vector, $u \in \mathbb{R}^n$ the input vector, $y \in \mathbb{R}^l$ the output vector. The mappings $A(\theta)$, $B(\theta)$, $C(\theta)$, $D(\theta)$ are affine functions of $\theta(t)$. The measurable parameter vector $\theta(t)$ represents a time-varying parameter vector referred to as scheduling signal vector, which is assumed to be confined to a compact set:

$$\theta(t) \in \mathscr{P} \subset \mathbb{R}^l, \forall t > 0$$

This section presents an LPV model of the vehicle lateral dynamics in the form of $G(\theta)$.

The time-varying parameter θ varies in a polytope $\mathscr{P}$ with vertices ω_1, ω_2, ..., ω_r. An LPV model is called polytopic if it can be presented by a convex combination of a finite number of state space matrices of the LPV model at vertices of $\theta(t)$. A matrix polytope is defined as a convex hull of these matrices [3], as

$$\left[\begin{array}{cc} A(\theta) & B(\theta) \\ C(\theta) & D(\theta) \end{array} \right] \in Co \left\{ \left[\begin{array}{cc} A_i & B_i \\ C_i & D_i \end{array} \right], i = 1, 2, ...r \right\}$$

$$= \sum_{i=1}^{r} \alpha_i \left[\begin{array}{cc} A_i & B_i \\ C_i & D_i \end{array} \right] : \alpha_i \geq 0, \sum_{i=1}^{r} \alpha_i = 1$$

where Co denotes the convex combination among systems at vertices.

Here, the state space matrices of the vehicle lateral dynamics can be regarded as fixed functions of two varying parameters which depend on the vehicle velocity $v_x(t)$:

$$\theta(t) = \left[\frac{1}{v_x(t)} \quad \frac{1}{v_x^2(t)} \right]^T.$$

B. 2-DOF LPV Controller Synthesis

In order to maintain stability and high performance along all trajectories of $\theta(t)$, the controller needs to be capable of adjusting to the variations in the plant dynamics. LPV gain scheduling is employed in this paper to synthesize the controller. With the existence of a quadratic Lyapunov function for all $\mathscr{P}$, the designed controller guarantees stability and a level of control performance along all admissible trajectories. The synthesis problem reduces to solve a system of linear matrix inequalities (LMIs), see [3].

We choose the yaw rate $\dot{\psi}$ as the measured output y, two states $x = [\beta \quad \dot{\psi}]^T$, and the steering angle δ as an exogenous input w, yaw torque M_z as the control input u. The controller is synthesized by shaping mixed sensitivities: sensitivity S and control sensitivity KS are designed to achieve desired properties of the closed-loop transfer function from the desired yaw movement $\dot{\psi}$ to the fictitious output vector $z = [z_s \quad z_k]^T$ [11]. The design is carried out by choosing suitable weighting filters W_s and W_k. The generalized plant

$P(s)$ is shown in Fig. 2. Its state space representation is given as:

$$\begin{aligned} \dot{x} &= A(\theta)x + B_1(\theta)w + B_2(\theta)u \\ z &= C_1(\theta)x + D_{11}(\theta)w + D_{12}(\theta)u \\ y &= C_2(\theta)x + D_{21}(\theta)w + D_{22}(\theta)u \end{aligned} \tag{4}$$

In order to be able to use the design techniques in [3], a

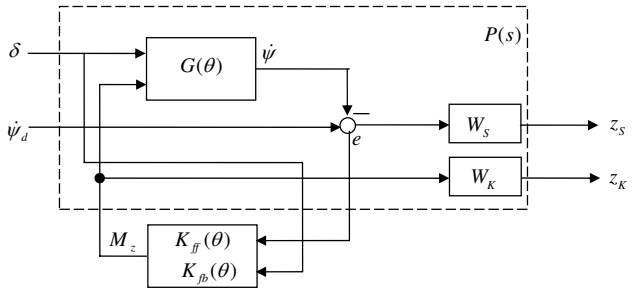

Fig. 2. Generalized plant with 2 DOF

prefilter is added to remove the parameter dependence of $B_2(\theta)$.

Here, to fulfill requirements of both reference tracking and disturbance rejection, a 2-DOF synthesis structure is employed. The controller $K(\theta)$ has the form:

$$\dot{x_k} = A_k(\theta)x_k + B_{ke}(\theta)e + B_{k\delta}(\theta)\delta \tag{5}$$

$$u = C_k(\theta)x_k + D_{ke}(\theta)e + D_{k\delta}(\theta)\delta \tag{6}$$

It has two inputs: steering angle δ as the reference, and the difference e between desired and measured yaw rate. The control output is the yaw moment M_z. The controller $K(\theta)$ can be decomposed into two parts: a feedforward controller $K_{ff}(\theta)$ to track the reference, and a feedback controller $K_{fb}(\theta)$ to reduce the errors due to disturbances and uncertainties. The two controllers are synthesized simultaneously in one optimization step.

C. Torque Distribution

The control output M_z is the torque needed at the center of gravity to generate yaw movement of the vehicle and has to be calculated for individual wheels. For this purpose, the dynamics of a dual track vehicle model is applied. Two variables σ and ρ are defined to relate the force requests of front and rear wheels $F_{x,F}$, $F_{x,R}$ and axis-force differences $\triangle F_{x,F}$, $\triangle F_{x,R}$ as:

$$F_{x,R} = \sigma F_{x,F} \tag{7}$$

$$\triangle F_{x,R} = \rho \triangle F_{x,F} \tag{8}$$

Depending on σ, it is possible to drive purely by ICE (σ = 0) or purely by electric motor ($\sigma = \infty$) or a combination. Setting $\rho \to \infty$, no torque difference at the front axle is required. Thus ICE driven wheels are in use.

So the resulting force on each wheel is expressed as [6]

$$\begin{aligned} F_{x,FL} &= F_{x,F} - \triangle F_{x,F} \\ &= \frac{F_x}{2(1+2\sigma)} - \frac{M_z}{\omega_F + \rho\omega_R} \end{aligned} \tag{9}$$

$$\begin{aligned} F_{x,FR} &= F_{x,F} + \triangle F_{x,F} \\ &= \frac{F_x}{2(1+2\sigma)} + \frac{M_z}{\omega_F + \rho\omega_R} \end{aligned} \tag{10}$$

$$\begin{aligned} F_{x,RL} &= F_{x,R} - \triangle F_{x,R} \\ &= \frac{F_x\sigma}{2(1+2\sigma)} - \frac{\rho M_z}{\omega_F + \rho\omega_R} \end{aligned} \tag{11}$$

$$\begin{aligned} F_{x,FR} &= F_{x,F} + \triangle F_{x,F} \\ &= \frac{F_x\sigma}{2(1+2\sigma)} + \frac{\rho M_z}{\omega_F + \rho\omega_R} \end{aligned} \tag{12}$$

D. Anti-Windup Control Scheme

An important design issue is actuator saturation, when the actuator capacity is limited by inherent physical constraints and limitations of the actuator. In this work, the maximum torque applied to each wheel is bounded either by the maximum applicable torque T_{eMot} or by the maximum power P_{eMot}, see Table I.

An anti-windup control scheme proposed in [4] is adopted here for the feedback control loop. The anti-windup scheme is constructed after the LPV self-scheduled controller is synthesized. The prerequisite to apply such a scheme is that, the matrix $D_{ke}(\theta)$ is invertible $\forall\theta(t) \in \mathscr{P}$. The feedback controller has the form:

$$\dot{x}_{ke} = A_k(\theta)x_{ke} + B_{ke}(\theta)e \tag{13}$$

$$u_e = C_k(\theta)x_{ke} + D_{ke}(\theta)e \tag{14}$$

where u_{ke} and x_{ke} are the output and states of the decomposed feedback controller, respectively.

By multiplying (14) with a matrix $H(\theta)$ and substracting from (13), we obtain

$$\begin{aligned} \dot{x}_{ke} =& (A_k(\theta) - H(\theta)C_k(\theta))x_{ke} \\ &+ (B_{ke}(\theta) - H(\theta)D_{ke}(\theta))e + H(\theta)u_e \end{aligned} \tag{15}$$

$$u_e = C_k(\theta)x_{ke} + D_{ke}(\theta)e. \tag{16}$$

Selecting $H(\theta) = B_{ke}(\theta)D_{ke}^{-1}(\theta)$ and replacing the controller output u_e with the saturated plant input $\tilde{u}_e$, the state space model of the controller can be written as follows.

$$\begin{aligned} \dot{x}_{ke} =& (A_k(\theta) - B_{ke}(\theta)D_{ke}^{-1}(\theta)C_k(\theta))x_{ke} \\ &+ B_{ke}(\theta)D_{ke}^{-1}(\theta)\tilde{u_e} \end{aligned} \tag{17}$$

$$u_e = C_k(\theta)x_{ke} + D_{ke}(\theta)e \tag{18}$$

The new structure of the feedback controller is shown in Fig. 3.

IV. Simulation Results

A 14-DOF vehicle model is employed for simulation use, see [6]. Among them, 6-DOF come from the center of gravity moving and rotating in all directions. 4-DOF are reserved for the suspension of the vehicle, the other 4-DOF for the

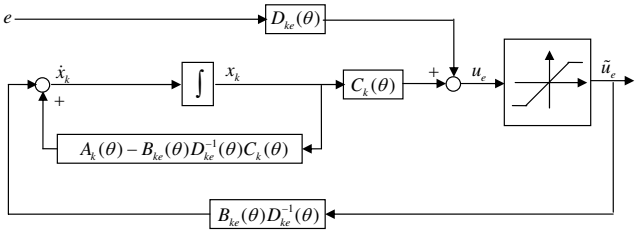

Fig. 3. Feedback control scheme with anti windup

TABLE I
PARAMETERS OF THE SIMULATION MODEL

a_f	1.24	distance from front axle to COG in m
a_r	1.228	distance from rear axle to COG in m
C_f	78972	Cornering stiffness of the front wheel in N/rad
C_r	79918	Cornering stiffness of the rear wheel in N/rad
ω_F	1.4450	width of the front axle in m
ω_R	1.4510	width of the rear axle in m
m	1500	mass of the vehicle in $kg \cdot m^2$
I_z	3263	moment of inertia around vertical axis in kg
T_{eMot}	775	maximal torque of one electric motor in Nm
P_{eMot}	50	maximal power of one electric motor in Kw
μ	1	adhesion coefficient between wheel and road

angular movement of the wheels. The tire characteristics are approximated by a modified Dugoff model [5]. Moreover, σ and ρ are chosen to be zero. The vehicle is rear-wheel-driven by an ICE, while two electric motors are installed on front wheels. The vehicle parameters used for simulation are listed in Table I.

A. Reference Generation

The yaw rate is one of the important state variables that describe the lateral motion of a vehicle. In this paper, the desired yaw rate $\dot{\psi}_d$ is chosen as the reference input according to inputs given by the driver: vehicle velocity v_x, and steering wheel angle that is directly related with steering angle at wheels δ by a steering ratio. The reference input is generated by an observer, see [6].

B. Implementation of the 2-DOF LPV Controller

There are two dependently varying parameters $\theta = [1/v_x(t) \quad 1/v_x^2(t)]^T$. Given the varying range of vehicle velocity $v_{xmin} = 1m/s$ and $v_{xmax} = 35m/s$, they form a parameter box with 4 vertices ω_1, ω_2, ω_3 and ω_4, where:

$$\omega_1 := \begin{bmatrix} 1/v_{xmin} \\ 1/v_{xmin}^2 \end{bmatrix}, \omega_2 := \begin{bmatrix} 1/v_{xmax} \\ 1/v_{xmin}^2 \end{bmatrix},$$

$$\omega_3 := \begin{bmatrix} 1/v_{xmin} \\ 1/v_{xmax}^2 \end{bmatrix}, \omega_4 := \begin{bmatrix} 1/v_{xmax} \\ 1/v_{xmax}^2 \end{bmatrix}.$$

However, this parameter box with four vertices introduces conservatism into the design: Among four vertices, it can be easily seen that, ω_2 is not reachable for any value of v_x. Hence, the polytope $\mathscr{P}$ is reduced to a triangle with vertices ω_1, ω_3 and ω_4 shown in Fig. 4, though there still remains some conservativeness on the polytope [12]. By solving the LMIs using Robust Control Toolbox of Matlab, a polytopic LPV controller is synthesized. W_s and W_k are filters to

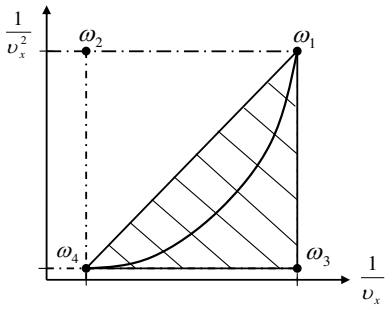

Fig. 4. Polytope of θ

shape the sensitivity and control sensitivity, respectively. By taking bandwidth, steady state error and control effort into consideration, the two filters are tuned as:

$$W_s = \frac{3 \times 10^6}{10^5 s + 1}, \quad W_k = \frac{1100s + 10^5}{5000s + 5 \times 10^9}.$$

The resulting LPV controller has an order of five.

C. Implementation of a Flat Feedforward and LQG Feedback Controller

The LPV controller is compared with a flatness-based controller in [6], where a flat feedforward control in combination with a PID and a Linear Quadratic Gaussian (LQG) feedback control for a TtR-HEV via torque vectoring is proposed to generate the desired force F_x in longitudinal direction and the desired yaw moment M_z. The longitudinal force F_x is needed to fulfill the prerequisites to construct a flat system. Apart from flat feedforward control, the feedback part is realized by combining PID and LQG. The input of the PID controller is the difference between desired and measured vehicle velocity v_x; the output is the longitudinal force F_x. The LQG controller corrects the error of the yaw rate $\dot{\psi}$. Its structure is shown in Fig. 5. It stabilizes the vehicle response in tracking tests.

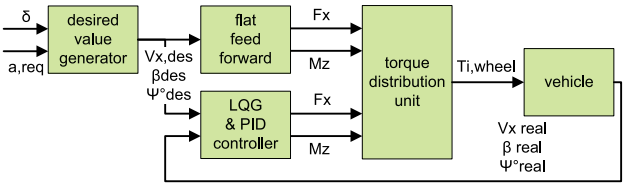

Fig. 5. Flatness-based control scheme

D. Comparison

To compare the performance of the two control schemes, several driving maneuvers are designed for testing.

i) Constant reference velocity with sinusoidal steering: In this driving maneuver, the reference vehicle velocity maintains 80 Kph. The sinusoidal steering has an amplitude of 120^o and frequency 0.7 Hz. At the valley of the sinusoidal curve, the steering wheel is held constant for 0.5 seconds before completing the

period. The simulation results are plotted in Fig. 6. Fig. 7 refers to the generated torque by feedforward and feedback controllers, respectively. The control input M_z is calculated as the sum of both torques.

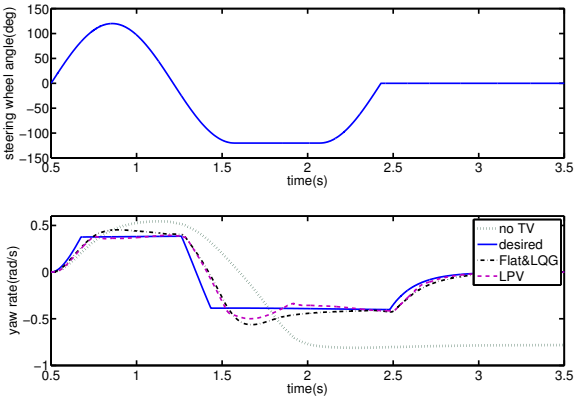

Fig. 6. Sensitivity (above) and control sensitivity (below) and constraints

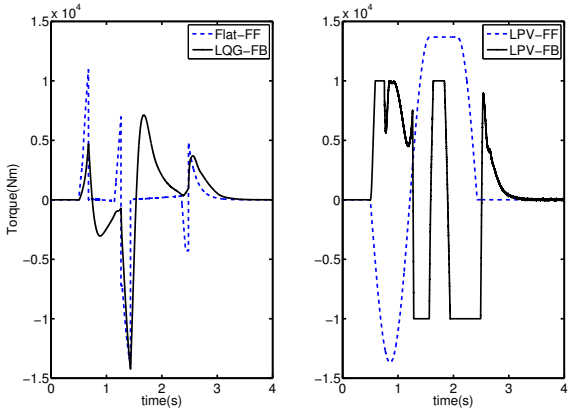

Fig. 7. Generated torque by flatness-based and LPV controllers respectively

ii) Normal driving behavior: Apart from above extreme driving situation, vehicles drive within the linear range most of the time. To test the performance of both controllers, some measured driver inputs are used to represent normal driving behavior. As shown in Fig. 8, first two rows are vehicle velocity and steering wheel angles given by the driver, the third row is the comparison between the desired yaw rate generated by the observer and the simulated yaw rate controlled by two controllers. Fig. 9 shows enlarged parts of the comparison for better visualization.

iii) Step steering with disturbance rejection: The foregoing two driving maneuvers demonstrate the performance of both controllers in reference tracking. To test their performance in disturbance rejection, we let the friction coefficient between the road and tires be subject to noise. The foregoing maneuvers are implemented under the assumption that vehicles drive on an ideal dry asphalt road, which indicates the friction coefficient 1.

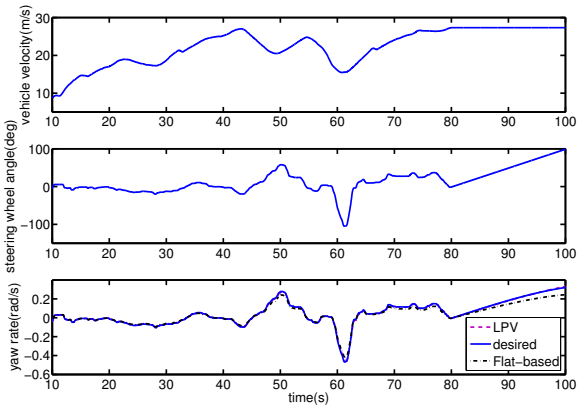

Fig. 8. Controlled yaw rate in normal driving

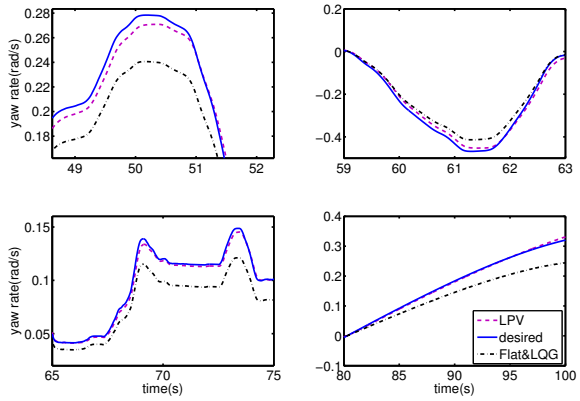

Fig. 9. Enlarged yaw rate comparison

The driving maneuver is defined as: a step steering of 80^o at 100 Kph. Meanwhile, measurement noise, simulated by an additive white Gaussian noise, is introduced along the whole driving, as shown in Fig. 10. The controller is expected to guarantee stability and accuracy against errors.

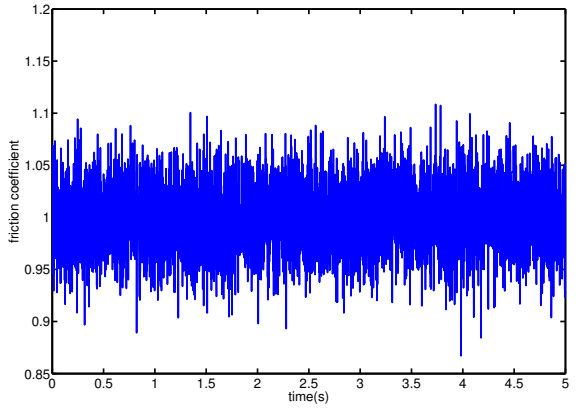

Fig. 10. noisy friction coefficient with Gaussian noise

Fig. 11 shows the comparison of vehicle responses by means of the LPV control and flatness-based control. Torques generated by feedforward and feedback controllers are shown in Fig. 12.

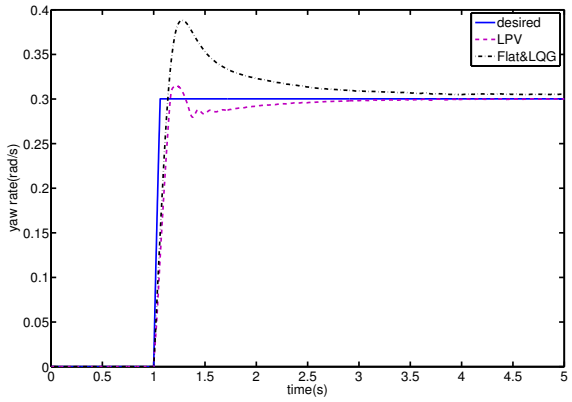

Fig. 11. The yaw rate comparison under disturbance

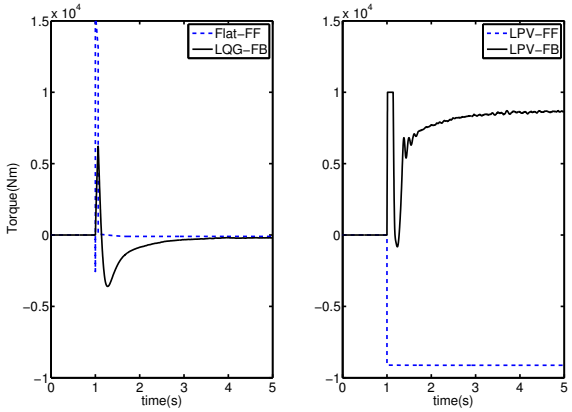

Fig. 12. Generated torque by flatness-based and LPV controllers respectively

E. Assessment of Simulation Results

Driving maneuver i) tests the performance of controllers in an extreme driving situation, where the vehicle drives at a relative high velocity and an abrupt change of steering may lead the vehicle out of control. It needs to be emphasized that both controllers are synthesized based on a simple linearized vehicle model and implemented to a more complex and realistic nonlinear model. Even though the vehicle handling largely violates the assumption of the single-track model, the stability of the closed-loop system is still guaranteed by both LPV and flatness-based controllers. Compared to the flatness-based controller, the LPV controller outperforms with smaller overshoot.

Both driving maneuvers i) and ii) are implemented for reference-tracking test. By taking external disturbance and simulation error into consideration, driving maneuver iii) is aimed at testing the robustness of the two controllers. As depicted in Fig. 11, the 2-DOF LPV controller achieves much smaller overshoot and steady state error with the presence of noise. Its feedforward and feedback controllers work together in an optimal way to realize high performance in both reference tracking and disturbance rejection tests. Moreover, the 2-DOF LPV controller is derived, by tuning one filter for sensitivity and one filter for control sensitivity, instead of tuning both filters for feedforward and feedback controllers separately. This control scheme can be easily and efficiently tuned and implemented.

V. Conclusions and Future Work

This paper presents a successful application of a 2-DOF LPV self-scheduled controller design of a TtR-HEV via torque vectoring. A feedforward and a feedback controller are synthesized in one step to achieve good tracking and high robustness against disturbances and modeling errors. An anti-windup control scheme is adopted to avoid significant performance degradation, when the actuator saturation occurs. By testing the designed controller in different driving maneuvers and comparing it with a flatness-based controller, its high performance and robustness have been demonstrated by simulation results. The controller designed in this paper is based on a simplified vehicle model - single track model. Further work can be implemented by adopting a more realistic 2-track model.

References

[1] C. C. Chan, K. T. Chau, *Modern Electric Vehicle Technology*, Oxford University Press, USA, 2001

[2] B. Chretien, F. Holzmann, G. Kaiser, S. Glaser, and S. Mammar, Concept of Through the Road Hybrid Vehicle, *Advanced Vehicle Control*, AVEC, Ed., Loughborough, 2010

[3] P. Apkarian, P. Gahinet, G. Becker, Self-scheduled H_∞ Control of Linear Parameter-varying Systems: a Design Example, *Automatica*, vol 31, no.9, 1995, pp.1251-1261

[4] H. P. Luedders, H. Abbas, D. Doberstein, F. Thielecke, H. Werner, LPV Gain-Scheduling Control of an Electromechanically Driven Landing Gear for a Commercial Aircraft, In *Proceedings of the 2010 American Control Conference*, MD, USA, June 30-July 02, 2010, pp. 4659-4664

[5] G. J. Forkenbrock, An Overview of NHTSA's 2005 ESC Research Program, 2005

[6] G. Kaiser, F. Holzmann, B. Chretien, M. Korte, H. Werner, Torque Vectoring with a Feedback and Feed Forward Controller - Applied to a through the Road Hybrid Electric vehicle, *IEEE Intelligent Vehicle*, Karlsruhe, 2011

[7] M. Burgess, Torque Vectoring, *Lotus Engineering*, [http://www.vehicledynamicsinternational.com]

[8] H. B. Pacejka, Tyre and Vehicle Dynamics, *Elsevier Butterworth-Heinemann*, 2002

[9] D. Bianchi, A. Bori, G. Burgio, M. D. Di Benedetto, S. Di Gennaro, Adaptive Integrated Vehicle Control Using Active Front Steering and Rear Torque Vectoring, In *Proceedings of the Joint 48th IEEE Conference on Decision and Control and 28th Chinese Control Conference*, Shanghai, China, December 16-18, 2009, pp. 3557-3562

[10] R. Rothfuss, J. Rudolph, M. Zeitz, Ein Neuer Zugang zur Steuerung und Regelung Nichtlinearer Systeme, *Automatisierungstechnik 45*, 1997, pp. 517-525

[11] S.Skogestad, I.Postlethwaite, Multivariable Feedback Control: Analysis and design, *John Wiley and Sons*, 2001

[12] A.Kwiatkowski, H.Werner, PCA-Based Parameter Set Mappings for LPV Models With Fewer Parameters and Less Overbounding, *IEEE Transactions on Control Systems Technology*, 2008